

# Ironmaking & Steelmaking

Processes, Products and Applications

ISSN: (Print) (Online) Journal homepage: <https://www.tandfonline.com/loi/yirs20>

## Suitability of pulverised coal testing facilities for blast furnace applications

Markus Bösenhofer , Eva-Maria Wartha , Christian Jordan , Christoph Feilmayr , Hugo Stocker , Franz Hauzenberger , Johannes Rieger , Stefan Tjaden , Arleen Walk & Michael Harasek

To cite this article: Markus Bösenhofer , Eva-Maria Wartha , Christian Jordan , Christoph Feilmayr , Hugo Stocker , Franz Hauzenberger , Johannes Rieger , Stefan Tjaden , Arleen Walk & Michael Harasek (2020) Suitability of pulverised coal testing facilities for blast furnace applications, Ironmaking & Steelmaking, 47:5, 574-585, DOI: [10.1080/03019233.2019.1565152](https://doi.org/10.1080/03019233.2019.1565152)

To link to this article: <https://doi.org/10.1080/03019233.2019.1565152>



© 2019 The Author(s). Published by Informa UK Limited, trading as Taylor & Francis Group



Published online: 20 Jan 2019.



Submit your article to this journal [↗](#)



Article views: 1351



View related articles [↗](#)




View Crossmark data [↗](#)



Citing articles: 3 View citing articles [↗](#)

## Suitability of pulverised coal testing facilities for blast furnace applications

Markus Bösenhofer <sup>a,b</sup>, Eva-Maria Wartha<sup>a</sup>, Christian Jordan<sup>a</sup>, Christoph Feilmayr<sup>c</sup>, Hugo Stocker<sup>d</sup>, Franz Hauzenberger<sup>e</sup>, Johannes Rieger<sup>b</sup>, Stefan Tjaden<sup>b</sup>, Arleen Walk<sup>b</sup> and Michael Harasek <sup>a</sup>

<sup>a</sup>Institute of Chemical, Environmental & Bioscience Engineering, Technische Universität Wien, Vienna, Austria; <sup>b</sup>K1-MET GmbH, Linz, Austria; <sup>c</sup>voestalpine Stahl GmbH, Linz, Austria; <sup>d</sup>voestalpine Stahl Donawitz GmbH, Leoben, Austria; <sup>e</sup>Primetals Technologies Austria GmbH, Linz, Austria

### ABSTRACT

Identifying coals suitable for blast furnace injection has become increasingly important due to rising injection rates. This review of traditional pulverised coal reactivity testing equipment reveals that no agreed-upon evaluation standard exists and that different reactor types are employed for testing. Therefore, reference blast furnace conversion conditions are defined, followed by a discussion of their influence on the coal conversion process as illustrated by conceptual conversion models. Critical process parameters are temperature, heating rate and pressure, while other effects can be calibrated. Evaluating the currently employed test equipment with regard to these process parameters shows that only specially designed drop-tube furnaces and flow reactors provide conversion conditions near to blast furnace conditions. For consistent injection coal testing, special reactors complying with the previously defined critical process parameters must be established.

### ARTICLE HISTORY

Received 25 September 2018  
Revised 21 December 2018  
Accepted 31 December 2018

### KEYWORDS

Pulverised coal injection (PCI); coal conversion; auxiliary reducing agents; blast furnace; iron making; design criteria; coal reactivity characterisation

### Introduction

Injecting pulverised coal (PC) into blast furnace raceway zones has become a popular approach to reduce metallurgic coke consumption. The best available techniques (BAT) document for the European Union's iron and steel industry [1] qualifies this direct injection of hydrocarbons as a promising technology to increase efficiency and reduce greenhouse gas emissions from blast furnaces. All forms of hydrocarbons reduce the metallurgic coke consumption and the gross energy consumption, e.g. by 3.6% at PC injection rates of 180 kg/t<sub>HM</sub> [1].

Metallurgic coke and PC compete for a limited amount of oxygen; therefore, high conversion rates and high PC consumption reduce the metallurgic coke consumption in the vicinity of the tuyeres. The disadvantage of direct injection is a decrease in the raceway temperature, which must be compensated by feeding O<sub>2</sub> into the hot blast. The maximum coal injection rate is believed to be somewhere around 270 kg/t<sub>HM</sub> as a consequence of thermo-chemical and coke/burden permeability reasons [1]. Although various hydrocarbons can be used for direct injection, this work focuses on (pulverised) coal. PC is fed into the hot blast a few centimetres upstream from the tuyere opening. Hot blast is typically a pre-heated oxygen-enriched air stream at temperatures of around 1200°C. Immediately after the PC leaves the cooled and inertised injection lance, particles are subject to intense heating, which starts thermo-chemical conversion processes. In general, the conversion of coal consists of following sub-processes [2,3]:

- drying,
- devolatilisation,
- volatiles combustion,
- gasification, and
- burnout.

The initial step of the coal conversion process involves drying and is followed by devolatilisation. During

devolatilisation, volatile compounds degas from the solid carbon matrix within the coal particle. The volatiles diffuse to the particle surface and are eventually transferred to the bulk gas phase, where they ignite if the bulk temperature exceeds their auto-ignition temperature and sufficient O<sub>2</sub> is available. Devolatilisation leaves a solid matrix called char. The volatile flame surrounding the coal particles releases CO, CO<sub>2</sub>, H<sub>2</sub>O, and H<sub>2</sub>, which interact with the carbon matrix through gasification reactions. When O<sub>2</sub> becomes available at the residual char's surface, char burnout starts. Burnout and gasification differentiate only by the involved gaseous reactants, but the complex mechanism of gas–solid reactions is the same. Gas–solid reactions generally consist of several distinct and simultaneously occurring steps [4]:

- Mass transfer of the gaseous reactant from the bulk gas phase to the external solid fuel surface.
- Intra-particle processes:
  - mass diffusion of the gaseous reactant from the external surface to the actual reaction site;
  - adsorption of the gaseous reactant to the reaction site;
  - chemical reaction of the adsorbed gaseous reactant and the solid;
  - desorption of the gaseous product from the reaction site;
  - mass diffusion of the gaseous product from the reaction site to the external surface.
- Mass transfer of the gaseous product from the external surface to the bulk gas phase.

Gasification and burnout steps are critical for the overall conversion time of coal particles [3], and both can be limited either by mass transfer from the gas phase to the reaction site or the chemical kinetic. Recent results suggest that even the coal preparation process, e.g. milling or grinding,

**Table 1.** Analysis results of common chemical coal evaluation methods [2, 3, 15].

Ultimate analysis	Proximate analysis	Petrographic analysis
C, H, N, S, O, ash	Volatiles, fixed carbon, ash, moisture	Vitrinite, inertinite, liptinite

affects the coal conversion process by changing surface chemistry and mineral phases [5].

In order to obtain comprehensive evaluation results of PCs and their applicability to blast furnaces, the employed test equipment should reproduce the fundamental features of the pulverised coal injection (PCI) process. Currently, PC performance in blast furnaces is evaluated in diverse equipment or test reactors. However, aside from Li et al. [6, 7], limited literature questions the applicability to reproduce blast furnace conditions. Because current knowledge indicates that coal conversion is decisively influenced by conversion conditions [2, 3, 8–14], evaluating coals under different operation conditions is assumed to significantly alter the outcome. Coals evaluated as suitable may cause problems when applied to the blast furnace and suitable coals might be rejected because of misleading evaluation results.

In addition to the burnout within the raceway zone, chemical composition also plays an important role in ensuring proper blast furnace operation and product qualities. Impurities such as sulphur, phosphor, chlorine and zinc can reduce pig iron quality. Therefore, potential injection coals must undergo chemical analysis. Standard tests for this are ultimate and proximate analysis, whereas petrographic analysis is a more advanced

analysis method. Petrographic analyses investigate the petrological composition (macerals) of coals, where macerals are comparable to minerals in the context of rocks [15]. Table 1 summarises common results from the three analysis methods.

This work aims to identify the potential key parameters to reproduce raceway zone conditions in test equipment. First, representative raceway conditions are discussed and, subsequently, the coal conversion process and its dependence on the surrounding conditions is evaluated. Next, the currently employed testing equipment is discussed and its applicability to reproduce raceway conditions is evaluated.

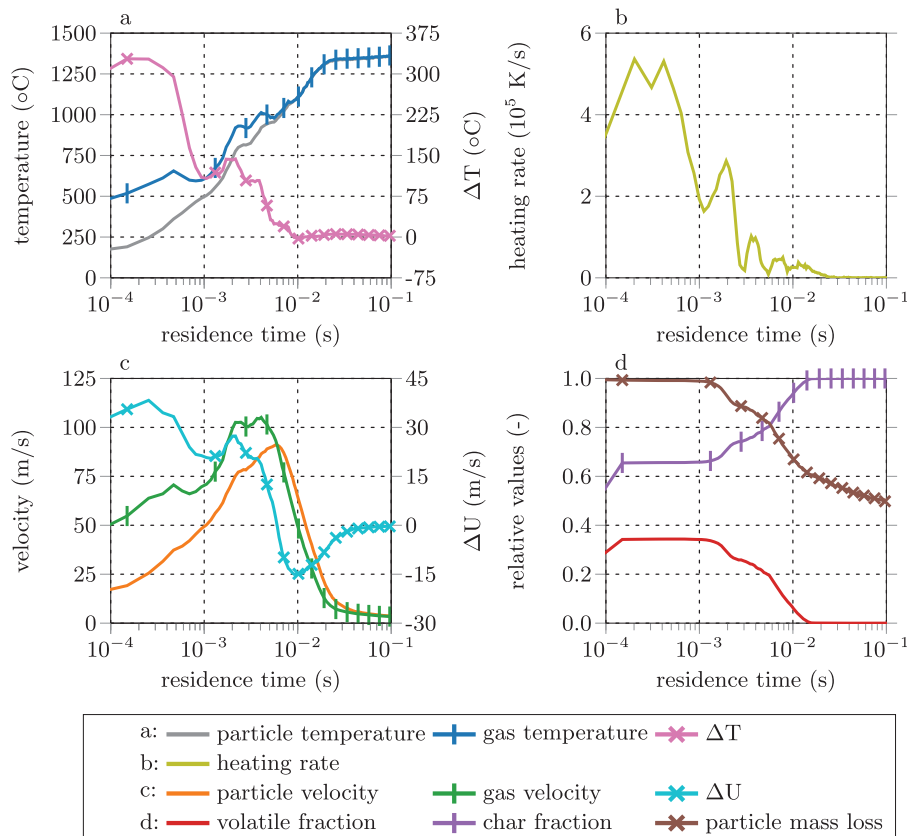
## Defining raceway conditions

PC conversion in the raceway zone is a process characterised by harsh conditions. Table 2 provides a generic set of the conditions in the current blast furnace raceway zones. The high temperatures and heating rates significantly influence the PC conversion process [7, 19–21]. Moreover, temperature, pressure, and velocity affect the species transport from the bulk gas phase to the coal surface, and from the surface to the actual reaction site. The given residence time indicates a typical time span available for converting PC in the oxygen-rich zone surrounding the tuyeres. The effects of the different process parameters are discussed separately in the following sections.

Figure 1 shows representative modelling results for the thermo-chemical coal conversion within the raceway zone for temperatures (a), heating rates (b), velocities (c), and

**Table 2.** Generic conditions for pulverised coal conversion within the blast furnace raceway zone [16–18].

Temperature range	Heating rates	Pressure	Hot blast velocity	Particle velocity	Flow type	Residence time
1200–2500°C	$10^4$ – $10^6$ K/s	2–5 bar	$\approx 200$ m/s	$\approx 20$ m/s	Turbulent	20–30 ms


**Figure 1.** Typical simulation results for temperature (a), heating rate (b), velocity (c), and thermo-chemical conversion (d) profiles of pulverised coal injected into the blast furnace raceway zone [16, 17].

particle conversion characteristics (d) versus particle residence time [16, 17]. Hot blast and coal temperatures are around 1250 and 200°C at the coal injection point. Both temperatures increase to around 1400°C after 100 ms. Heating rates reach values up to  $6 \times 10^5$  K/s in the vicinity of the injection point and gradually decrease due to the thermal fluxes between particles and the surrounding fluid. Particle injection velocities are around 20 m/s, resulting in an initial gas–particle relative velocity of around 30 m/s. Gas and particles accelerate due to heat-up and the resulting gas phase expansion towards the raceway border. At the border, both are shown to slow down due to momentum exchange with the dense coke phase. The particle mass loss curve shows that only around 50% of the particle mass has been converted after 100 ms. However, volatile and char fractions indicate that only pyrolysis char enters the dense coke bed.

### Dependences of PC conversion

To isolate the effects of main operating parameters (temperature, pressure), heating rates, fluid–solid interface, and particle size on PC conversion, a theoretical analysis first describes well-established mechanistic modelling concepts to outline the dependences on coal conversion rates accompanied by literature challenging the analysis. This analysis is followed by a presentation of the key parameters for reproducing blast furnace operating conditions.

#### Temperature

Temperature directly affects the intrinsic reaction rate of hetero- and homogeneous reactions, which are typically modelled using the Arrhenius form. Pressure and concentration effects are incorporated by functional expressions [22]:

$$k_i(T, c) = k_0 \cdot \exp\left(\frac{-E_a}{RT}\right) \cdot f(c_1, c_2, c_3, \dots, c_N) \quad (1)$$

The parameters  $k_0$ ,  $E_a$  correspond to the Arrhenius parameters.  $R$  is the universal gas constant,  $T$  the temperature and  $c_i$  the species concentrations. Heterogeneous gas–solid reactions are more complex and consist of several steps, e.g. boundary layer diffusion, pore diffusion, adsorption, desorption, and the actual reaction. Because fuel particles can be of porous or dense nature, the actual reaction occurs either at the particle outer surface in case of dense fuel particles or at the particle inner surface in case of porous particles [4]. The effective or apparent reaction rate is the measurable rate and includes mass transfer effects, while the intrinsic reaction rate is the actual rate of adsorbed reactants and the solid matrix [2, 4].

Rumpel [23, 24] proposes a conceptual model for the gas–solid conversion of porous solids based on the contribution of diffusion sub-processes:

$$k_{i,eff}(T, c_i) = \frac{1}{\frac{1}{\beta \cdot a_{solid} \cdot c_{i,bulk}^{1-n}} + \frac{1}{\eta \cdot k_i}} \cdot c_{i,bulk}^n \quad (2)$$

Intrinsic rates are significantly affected by temperature. The first term in the denominator on the right-hand side of Equation (2) represents the contribution of the boundary layer diffusion from the bulk to the particle surface, while the second term represents the contribution of the pore

diffusion and the intrinsic reaction rate.  $\beta$  is the mass transfer coefficient between the surrounding and particle,  $a_{solid}$  is the total (inner and outer) specific particle surface, and  $c_{i,bulk}$  is the bulk concentration of the gaseous reactant. The intrinsic reaction rate  $k_i$  is corrected with the effectiveness factor  $\eta$  to account for pore diffusion effects during the particle conversion [23–25]. Both the mass transfer coefficient and the effectiveness factor depend on species diffusivity. The effects of temperature on the diffusion coefficients are also discussed later.

Mehrabian et al. [26] propose a conversion model for dense particles, assuming infinitesimal reaction layers moving from the solid surface to its centre, based on the layer approach proposed by Thunman et al. [27]:

$$k_{i,eff}(T, c_i) = \frac{1}{\frac{1}{\beta A_s} + \frac{1}{D_{i,eff}} \int_{r_r}^{r_s} \frac{dr}{A(r)} + \frac{1}{k_i A_r}} \cdot c_{i,bulk} \quad (3)$$

In this approach,  $A$  and  $r$  represent the area and the radial position of the surface  $s$  and the reaction layer  $r$ , respectively. The terms in the denominator denote the boundary layer diffusion rate, the pore diffusion rate and the actual reaction rate, respectively. In contrast to the model proposed by Rumpel [23, 24], Mehrabian et al. explicitly consider pore diffusion from the surface to the reaction side.

Diffusion within solid particles is controlled by molecular and/or Knudsen diffusion, depending on the ratio between the mean free molecule path ( $\lambda$ ) and the characteristic length scale ( $L_c$ ), i.e. the Knudsen number ( $Kn$ ):

$$Kn = \frac{\lambda}{L_c} = \frac{k_B * T}{\sqrt{2} \pi \sigma^2 \rho L_c} \quad (4)$$

Here,  $k_B$  is the Boltzmann constant,  $T$  is the temperature,  $\sigma$  is the molecule diameter, and  $L_c$  is the characteristic length, e.g. pore diameter.  $Kn$ , in the range of unity, characterises the transition regime between molecular and Knudsen diffusion, while molecular diffusion is predominant for  $Kn$  well below unity. In pore sizes above 100 nm, molecular diffusion is predominant, while Knudsen diffusion is dominant for pore sizes between 0.5 and 100 nm. An effective diffusion coefficient accounting for both regimes is employed in the transition regime [23, 24, 26]:

$$D_{eff,i} = \frac{1}{\frac{\tau}{D_{K,i}\epsilon} + \frac{\tau}{D_{M,i}\epsilon}} \quad (5)$$

Both diffusivities are corrected by the ratio of particle porosity ( $\epsilon$ ) and particle tortuosity ( $\tau$ ) to incorporate pore effects on diffusion rates [28]. Knudsen diffusion is a function of the pore size ( $d_{pore}$ ), the diffusing species' molecular weight ( $M_i$ ), the ideal gas constant ( $R$ ), and the temperature:

$$D_{K,i} = \frac{d_{pore}}{3} \sqrt{\frac{8RT}{M_i \pi}} \quad (6)$$

The molecular diffusion coefficient of specie  $i$  in the gas mixture ( $D_{M,i}$ ) is expressed, e.g. by the mixture rule proposed by Wilke [29]:

$$D_{M,i} = (1 - X_i) \left( \sum_{j \neq i} \frac{X_j}{D_{ij}} \right)^{-1} \quad (7)$$

In this mixture rule,  $X$  denotes the mole fraction of species  $i$  or  $j$  and  $D_{ij}$  is the binary diffusion coefficient of species  $i$  in  $j$ .

The binary diffusion coefficients are expressed by the solution of the Boltzmann equation assuming ideal gas as proposed by Chapman and Enskog [30]:

$$D_{ij} = \frac{3}{16} \frac{RT^{1.5} \sqrt{4\pi k_B}}{P \pi \sigma_{ij}^2 \Omega_D \sqrt{M_{ij}}} \quad (8)$$

The binary diffusion coefficients depend on  $T$ , the temperature-dependent collision integral ( $\Omega_D$ ), the pressure ( $P$ ), the molecular weights ( $M$ ), the characteristic length of the inter-molecular forces ( $\sigma$ ), and  $R$ .

Summarising the above points, temperature affects gas-solid conversion rates by changing the intrinsic reaction rates and the diffusion rates. Reaction rates depend exponentially on temperatures ( $k_j \propto e^{-1/T}$ ), while diffusion rate dependence is more complex. Knudsen diffusion increases with increasing temperature ( $D_{K,i} \propto T^{0.5}$ ), while the binary diffusion coefficients depend on temperature, with a more complex relation ( $D_{M,i} \propto T^{1.5}/\Omega_D(T)$ ) [30].

Since both mass transport from the bulk gas phase to the reaction site and the intrinsic conversion rates strongly depend on temperature, suitable experimental temperatures are necessary to obtain reliable results for the conversion behaviour of PC in blast furnaces.

### Heating rate

PC heating rates range between  $10^5$  and  $10^6$  K/s in the blast furnace raceway [16, 17]. Two distinct coal conversion effects can be associated with high heating rates: particle fragmentation [9–14] and an increased conversion/reactivity of inertinite [7, 19–21]. Investigations of inertinite rich coals revealed that the fusible (reactive) share increases at higher heating rates [7, 19–21]. An increased amount of fusible inertinite results in a more reactive pyrolysis char and higher conversion rates.

Fragmentation is reported to be caused either by thermal stresses due to intra-particle temperature gradients [11] or by internal pressure gradients from the volatiles emerging during devolatilisation [11, 13] or a combination of both. Literature indicates that vitrinite-rich coals are prone to fragmentation [9, 10, 12, 14] since vitrinite is one of the most brittle coal macerals [15]. Kim et al. [14] and Friedmann et al. [9, 10] investigate the fragmentation behaviour of different coal type particles, and both indicate a higher fragmentation probability for anthracite-like coals (high vitrinite content). Moreover, Friedmann et al. [9, 10] also indicate that fragmentation increases with increasing heating rates. Fragmentation due to thermal stresses significantly depends on the particle heating rates and the physical properties of the coal.

The probability of intra-particle gradients is characterised by the Biot number ( $Bi$ ), which denotes the ratio between the external and internal heat transfer of the fuel particle [28]:

$$Bi = \frac{L_c \cdot h_{eff}}{k_{solid}} \quad (9)$$

$L_c$  is a characteristic length, e.g. particle diameter, while  $h_{eff}$  is the effective heat transfer coefficient, including convective and radiation heat transfer from the surrounding to the particle surface, while  $k_{solid}$  is the thermal conductivity of the solid. If  $Bi$  is larger than unity, the heat transfer rate within the solid is lower than the heat transfer rate to the solid surface. Therefore, considerable intra-particle temperature

gradients occur. For  $Bi$  below unity, the uniform temperature assumption is valid and only minor temperature gradients occur. Biot numbers of coal particles within the blast furnace raceway zone are around unity directly after injection, depending on the physical coal properties and particle size [10, 16, 17].

The external pyrolysis number ( $Py$ ) compares the reaction and heat transfer time scales [31]:

$$Py = \frac{h_{eff}}{k_{py} \rho_{solid} c_{p,solid} L_c} \quad (10)$$

Here,  $k_{py}$  is the pyrolysis rate,  $\rho_{solid}$  is the solid density and  $c_{p,solid}$  is the solid heat capacity. If  $Py$  is above unity, the pyrolysis process is controlled by chemical kinetics, while heat transfer controls the process for  $Py$  below unity.  $Py$  within the blast furnace raceway zone depends on the coal reactivity and its physical properties. However, intense heat transfer by convection and radiation means that  $Py$  could exceed unity and the pyrolysis process might be reaction-controlled. Considering the high temperatures within the raceway, high pyrolysis rates occur, resulting in high gas generation rates within the solid matrix. Pressure gradients can arise that might lead to particle fragmentation, since diffusion rates of the pyrolysis gases to the particle surface are limited [9–14]. Therefore, a dimensionless number based on the reaction rate and internal mass diffusion rate of the pyrolysis gases, similar to the internal pyrolysis number, characterises the likeness of intra-particle pressure gradients [28]:

$$Ha = \sqrt{\frac{k_{py} L_c^2}{D_{eff}}} \quad (11)$$

$Ha$  is the Hatta number and  $D_{eff}$  is the smallest diffusion coefficient of the pyrolysis gases. If  $Ha$  is above unity, pressure gradients arising from high gas release rates are likely, while pressure gradients are negligible for  $Ha$  below unity. For typical blast furnace conditions,  $Ha$  could exceed unity. The actual values and fragmentation behaviour of coal particles are strongly dependent on the physical coal properties.

### Pressure

Ambient pressure affects the species transport from the bulk fluid to the reaction site, the intrinsic reaction rate, the fragmentation behaviour, product yields, and morphology during thermo-chemical coal conversion [8, 11]. At higher pressures, binary diffusion (Equation (8)) and effective diffusion rates decrease within the fluid and particle pores (Equation (5)). Mass diffusion rates are inverse proportional to the pressure ( $D \propto 1/P$ ) [30]. According to Wall et al. [8], higher partial pressures of gaseous reactants increase conversion rates of pyrolysis chars. Keeping the partial pressure constant while increasing the total pressure provides higher conversion rates up to a certain pressure. Above this threshold pressure, conversion rates decrease. Both observations are in line with the presented findings of the theoretical analysis: Total pressure increase decreases mass diffusivity, while a concentration increase increases mass fluxes and, thus, the conversion rates.

Intrinsic reaction rates depend on reactant species' partial pressures or concentrations, while adsorption rates to active surface reaction sites increase at higher partial pressures. The dependence of the intrinsic rate on the pressure is



proportional to the partial pressure of the educt species ( $k_{i,eff} \propto (X_i p)^n$ ).  $n$  incorporates non-linear effects in the adsorption process of the reactant to the active surface site, which are expressed as reaction order in kinetic modelling [2, 4].

The effect of the intra-particle pressure on the fragmentation behaviour has been studied by Stanmore et al. [11], among others. By varying the ambient pressure, they show that intra-particle pressure gradients affect fragmentation probability. They ascribe this to a reduced differential pressure between the interior and surrounding at elevated pyrolysis pressures. However, Wall et al. [8] report a decrease in pyrolysis gases, with a simultaneous increase of solid yields at elevated pressures. The reason for the lower fragmentation probability might be a combination of both effects. Wall et al. also report pressure effects such as smaller residual ash particles and reduced conversion duration at elevated pressures. A more detailed discussion of these issues can be found elsewhere [8, 11].

### Fluid–solid interface

Heat and mass transfer are dominated by the fluid surrounding the coal particles. Boundary layers for momentum (velocity/flow), heat and mass transfer emerge in the vicinity of particle surfaces [28, 32]. They develop according to fluid properties and the surrounding fluid flow situation. Boundary layers of these three transport phenomena are compared by dimensionless numbers, e.g. the Prandtl ( $Pr$ ), the Schmidt ( $Sc$ ), and the Lewis number ( $Le$ ).  $Pr$  relates to the fluid dynamic and heat transfer boundary layer. If  $Pr \ll 1$ , the heat transfer layer is thicker than the fluid dynamic one. The Prandtl number relates the kinematic viscosity ( $\nu$ ) and the thermal diffusion rate ( $\alpha$ ):

$$Pr = \frac{\nu}{\alpha} = \frac{\rho c_p \nu Le}{\kappa Sc} \quad (12)$$

The thermal diffusion rate is based on physical gas properties, where  $\rho$  is the bulk density,  $c_p$  is the specific heat capacity, and  $\kappa$  is the thermal conductivity. The Schmidt number relates to the fluid flow and mass transfer boundary layer and is expressed as the ratio of the kinematic viscosity and the mass diffusivity ( $D_{M,i}$ ):

$$Sc = \frac{\nu}{D_{M,i}} = \frac{Le}{Pr} \quad (13)$$

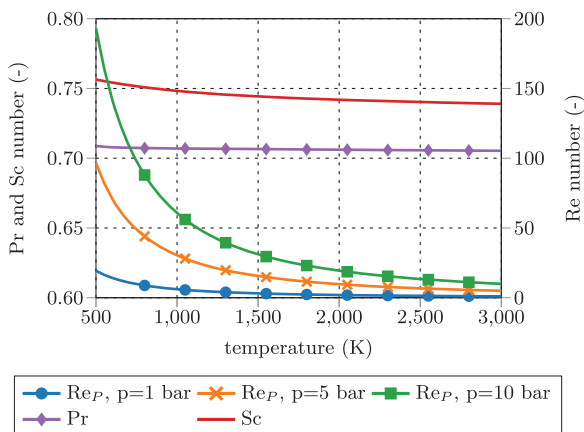


**Figure 2.**  $Pr$ ,  $Sc$ , and  $Re$  number versus temperature at blast furnace conditions.  $d_p = 75 \times 10^{-6}$  m,  $u_{rel} = 10$  m/s. Results are based on substance models from Cantera [33].

The Lewis number is the ratio of the thermal diffusivity and the mass diffusivity and relates the thermal and mass transport boundary layer thickness to each other:

$$Le = \frac{\alpha}{D_{M,i}} = \frac{Sc}{Pr} \quad (14)$$

For ideal gases at blast furnace conditions, the characteristic quantities are  $Pr \approx 0.7$ ,  $Sc \approx 0.7$ , and  $Le \approx 1$ . Figure 2 shows that  $Pr$  and  $Sc$  are in the estimated range for blast furnace conditions. In addition, it illustrates particle Reynolds numbers ( $Re_p$ ) as a function of temperature and pressure.

The convective and diffusive heat and mass transfer from the bulk to the particle surface are characterised by the Nusselt ( $Nu$ ) and Sherwood ( $Sh$ ) numbers, respectively. Both numbers are defined as the ratio of the actual transfer rate to the transfer rate in case of pure diffusion. They can be expressed by correlations of  $Re_p$  and  $Pr$  or  $Sc$ :

$$Re_p = \frac{u_{rel} d_p}{\nu} \quad (15)$$

$$Nu = \frac{h_{conv} L_c}{k_{fluid}} = f(Re_p, Pr) \quad (16)$$

$$Sh = \frac{\beta L_c}{D_{eff}} = f(Re_p, Sc) \quad (17)$$

$Re_p$  is defined as the ratio of the fluid–particle relative velocity, where ( $u_{rel}$ ) is the fluid–particle relative velocity,  $d_p$  is the particle diameter (characteristic length), and  $\nu$  is the fluid viscosity.  $k_{fluid}$  and  $h_{conv}$  are the thermal conductivity and the conductive heat transfer coefficients, respectively. The transfer rates depend on the transfer coefficients ( $h_{conv}$  and  $\beta$ ) and the temperature or concentration gradient between the bulk and the surface:

$$\dot{q}_{conv} = h_{conv} \Delta T \quad (18)$$

$$\dot{n}_{i,conv} = \beta_i \Delta c_i \quad (19)$$

Since  $Pr$  and  $Sc$  numbers are constant at raceway conditions,  $Nu$  and  $Sh$  depend solely on  $Re_p$ . By definition, the actual heat and mass transfer rates vary because of changes in the thermal conductivity or mass diffusivity caused by temperature and pressure variations. Therefore, the convective heat and mass transfer rates are proportional to the magnitude of the fluid–particle relative velocity ( $h_{conv} \propto \beta \propto u_{rel}$ ) and the magnitude of the gradient, e.g.  $\Delta T$  and  $\Delta c_i$ . The radiative heat flux from the bulk to the particle surface can be approximated by [28]

$$\dot{q}_{rad} = \sigma \epsilon (T_{surface}^4 - T_s^4) \quad (20)$$

Here,  $\sigma$  is the Stefan–Boltzmann constant,  $\epsilon$  is the emission coefficient,  $T_{surface}$  is the temperature of the surrounding surfaces (e.g. coke bed or furnace walls), and  $T_s$  is the particle surface temperature. Thus, the radiative heat transfer is proportional to the fourth power of  $T_{surface}$  ( $\dot{q}_{rad} \propto T_{surface}^4$ ).

### Particle size

Particle size has an influence on most of the above-discussed parameters. Effectiveness factors or pore diffusion from the particle surface to the reaction site depend on particle size (see Section ‘Temperature’). The characteristic length scale

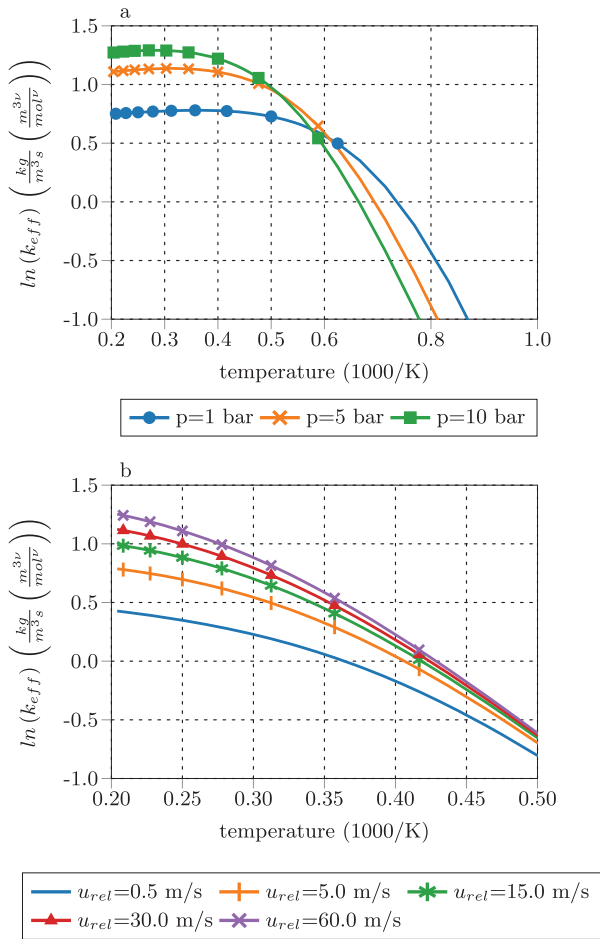


**Figure 3.** Effective reaction rate of a coal particle with  $O_2$  in air according to Equation (2) versus temperature and for different pressures (a) and temperature and different relative velocities (b). Particle properties were assumed as  $\epsilon = 0.5$ ,  $\tau = 0.6$ ,  $d_{pore} = 10^{-5}$  m,  $d_{coke} = 0.025$  m, and  $\rho_{coke} = 800$  kg/m<sup>3</sup>; Arrhenius parameters:  $k_0 = 3.87 \times 10^7$  kg/s,  $E_a = 150.5$  kJ/mol, and  $\nu_{O_2} = 0.59$  [23]; (a)  $U_{rel} = 15$  m/s, (b)  $p=5$  bar.

$L_c$ , which is the particle diameter for (almost) spherical particles, is relevant for the peculiarity of intra-particle temperature gradients ( $Bi$ ), pyrolysis regime ( $Py$ ), and the fragmentation probability ( $Ha$ ) as discussed in Section 'Heating rate'. Approximating the fluid–solid interface by the spherical surface indicates higher transfer rates for larger particles. However, the specific external surface is significantly larger for small particles and, thus, allows higher heat and mass transfer rates than for larger particles.

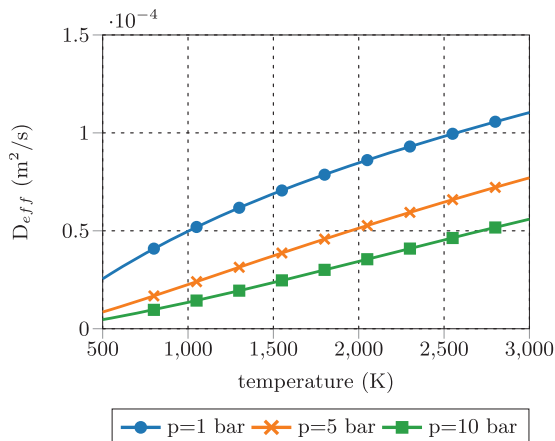


**Figure 4.** Effective diffusion coefficient of  $O_2$  in air versus temperature and for different pressures according to Equation (5). Particle properties were assumed as  $\epsilon = 0.5$ ,  $\tau = 0.6$ , and  $d_{pore} = 10^{-5}$ .

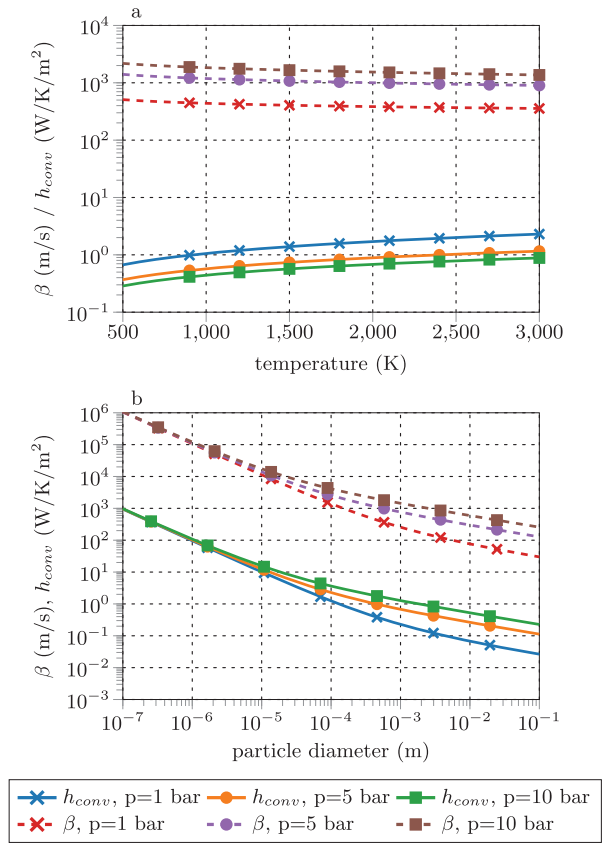


**Figure 5.** Heat transfer coefficients ( $h_{conv}$ ) and mass transfer coefficients ( $\beta$ ) of air and  $O_2$  mass transfer coefficient of a single spherical particle versus temperature and pressure (a) and versus particle diameter and relative velocity (b). (a)  $U_{rel} = 15$  m/s,  $d_{particle} = 0.025$  m; (b)  $T=2000$  K,  $p=5$  bar.

**Table 3.** Overview of the discussed coherences between experimental conditions and coal conversion characteristics.

Sub-process	Coherences
Intrinsic reaction rate	$e^{-1/T} \cdot f(p_i)$
Effective diffusion	$\frac{\tau^2}{T^{1.5+\Omega_p(T)-p}} \cdot \Delta C_i$
Boundary layer mass transfer	$u_{rel} \cdot \Delta C_i \cdot d_p^2$
Heat transfer (heating rates)	$(u_{rel} \cdot \Delta T_i + T_{bulk}^4) \cdot d_p^2$
Fluid physical properties	$f(T, P, c)$
Solid physical properties	$f(T, c)$

### Summary conversion effects

As discussed in the previous subsections, the intense conditions within the blast furnace raceway zone significantly affect the coal conversion characteristics. The combination of high temperatures, high heating rates, and elevated pressure pose challenges for designing suitable test reactors. Evaluating the involved processes in PC conversion, in turn, enables the evaluation of the contribution to the overall conversion process. For clarity, effective reaction and diffusion rates as well as heat and mass transfer coefficients are shown for typical conditions. Figure 3 visualises the dependences of the effective reaction rate (Equation (2)) on temperature, pressure, and relative velocity between gas and solid. Increasing temperature, pressure and relative velocity promotes coal conversion rates.

Figure 4 illustrates the effects of temperature and pressure on the diffusivity within porous coal particles. Effective  $O_2$  pore diffusivity of a solid particle in air is taken as an example. High temperatures and low pressures are favourable for diffusion rates. Coal properties significantly affect the pore diffusion rates [2, 3, 23, 24].

**Table 4.** Overview of selected institutions researching pulverised coal conversion (sorted by country).

Institution	Country	Method(s) <sup>a</sup>	Source
University of Newcastle, formerly BHP Billiton Newcastle Technology Center	Australia	IR	[7, 34–36]
Iron & Steelmaking Research Group – LASID, Technology Center, Federal University of Rio Grande do Sul	Brazil	TGA	[37]
Natural Resources Canada, CanmetENERGY	Canada	IR	[38]
Center for Innovation Competence Virtuhcon	Germany	DTF, FR	[39, 40]
Department of Ferrous Metallurgy, RWTH Aachen University	Germany	IR/FR, TGA	[18, 41–45]
Power Coal Division, Central Institute of Mining and Fuel Research (CSIR)	India	TGA,DTF	[46]
Materials & Processing Research Center/Applied Technology Research Center, NKK Corporation	Japan	IR	[47]
School of Mechanical Engineering, Pusan Clean Coal Center, Pusan National University	South Korea	FR	[14]
Energy Research Centre of the Netherlands (ECN)	The Netherlands	FR/DTF	[48, 49]
Institute of Thermal Technology, Silesian University of Technology	Poland	FR	[50, 51]
Centro Nacional de Investigaciones Metalurgicas (CSIC)	Spain	IR	[52]
Instituto Nacional del Carbon (INCAR)	Spain	DTF/IR	[53–55]
Luossavaara-Kiirunavaara AB (publ) mining corporation (LKAB)	Sweden	BF	[56]
Steel and Aluminum Research and Development Department, China Steel Corporation	Taiwan	DTF	[57]
Physical and Metallurgical Faculty, Donetsk National Technical University	Ukraine	IR	[43]
Coal Technology Research Group of Chemical, Mineral and Environmental Engineering, University of Nottingham	United Kingdom	DTF	[58]
Department of Chemical Engineering, Imperial College London	United Kingdom	WR	[21, 59–61]
Combustion Research Facility, Sandia National Laboratories	USA	FR/DTF	[62–64]

<sup>a</sup>DTF, drop-tube furnace; FR, flow reactor; IR, injection rig; TGA, thermo gravimetric analysis; WR, wire-mesh reactor.

Furthermore, Figure 5 shows the relations between heat and mass transfer coefficient and temperature, pressure, particle size, and relative velocity. It indicates a decrease of heat transfer coefficients at higher pressures, while mass transfer coefficients increase. This contradictory behaviour is caused by the physical fluid properties. Relative velocity and particle size have a more pronounced effect on heat and mass transfer than temperature and pressure. Since both transfer coefficients have been derived by employing the analogy between heat and mass transfer, they show a similar dependence on particle size and velocity. The lowest specific transfer rates occur at low relative velocities for large particles. Decreasing particle sizes and increasing relative velocities improves transfer rates.

In general, a higher specific surface causes smaller particles to react at higher rates than larger ones. Moreover, small particles tend to have insignificant intra-particle temperature

gradients and negligible fragmentation due to intra-particle pressure gradients (compare Sections 'Heating rate' and 'Pressure'). Table 3 sums up the identified coherences between the operation conditions and the coal conversion rate.

Test reactors should correctly reproduce the key operating parameters when screening coals for the application in the metallurgical industry. Based on the involved phenomena and the results of Table 3, the following parameter set has been identified:

- (blast) temperature,
- heating rate,
- pressure,
- particle size,
- gas–particle interface (boundary layer), and
- residence time.



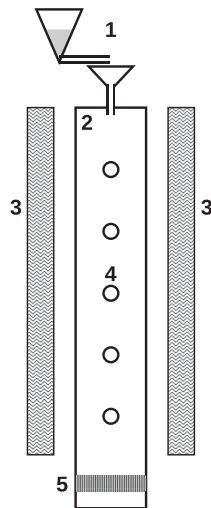


**Figure 6.** Schematic drop-tube furnace (DTF); 1, fuel feeder; 2, reactor; 3, heating elements; 4, sampling ports along reactor; 5, sampling at reactor end.

Recommended design criteria are process temperature, heating rates, and pressure. Remaining close to the actual blast furnace operating conditions ensures that all important conversion characteristics are preserved. It is also recommended to employ similar particle size distributions, although they are subject to proper sample pre-processing. Gas-particle interface and residence time are assumed to be of minor importance when designing a test reactor. Keeping gas-particle relative velocities at the injection point is expensive in terms of consumables, while they equalise in a short time. Both residence times and gas-particle interface effects can be calibrated by comparison with known coals.

### Current coal reactivity testing facilities and methods

This section outlines selected institutions active in the field of PC characterisation. Given this article's specific focus, the list is not exhaustive. In addition, institutions' employed testing methods are discussed and compared to the reference blast furnace operating conditions as defined in Section 'Defining raceway conditions'. Subsequently, their applicability for PC injection characterisation is evaluated.

#### Overview testing facilities

The following presents selected infrastructure employed for the characterisation of PCs with a special focus on blast furnace application, and is solely based upon available literature. PC characterisation equipment tends to be available worldwide. However, some institutions have a special focus on this specific topic. Table 4 summarises the institutions considered in this work.

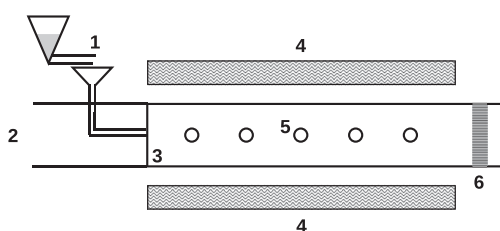


**Figure 7.** Schematic flow reactor (FR); 1, fuel feeder; 2, gas co-flow; 3, reactor; 4, heating elements; 5, sampling ports along reactor; 6, sampling at reactor end.

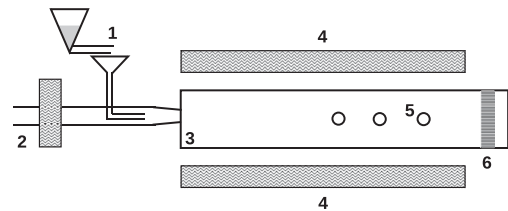


**Figure 8.** Schematic injection rig (IR); 1, fuel feeder; 2, blast pre-heater; 3, combustion chamber; 4, heating elements; 5, sampling ports along reactor; 6, sampling at reactor end.

Five different reactor concepts are employed for the lab-scale evaluation of PCI coals by the discussed institutions:

- drop-tube furnaces (DTF),
- flow reactors (FR),
- injection rigs (IR),
- thermo-gravimetric analysis (TGA), and
- wire-mesh reactors (WR).

### Coal reactivity testing methods

The following subsection briefly restates the different reactor types employed for the PC classification of Table 4 and summarises the capabilities of the employed equipment.

#### Drop-tube furnace

Drop-tube furnaces (DTF) are essentially vertical pipes heated from the outside, and solid samples pass the reactor due to gravitational acceleration. Particle and gas phase samples are typically taken at the reactor outlet or in a vertical direction along the reactor for varying residence times. The sample heating rates in DTFs range from  $10^4$  K/s, reaching maximum operation temperatures of up to  $1700^\circ\text{C}$  [57]. By probing through sampling ports, residence times may vary between several ms up to several seconds [54, 58]. Operation pressures of up to 100 bars are employed, with sample mass flow rates for DTFs ranging from  $10^{-3}$  up to 2 kg/h [7, 46]

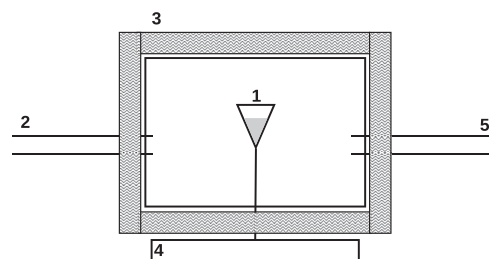


**Figure 9.** Schematic thermo-gravimetric analysis (TGA); 1, fuel sample; 2, pre-defined reaction gas; 3, external heating; 4, balance; 5, gas sampling.

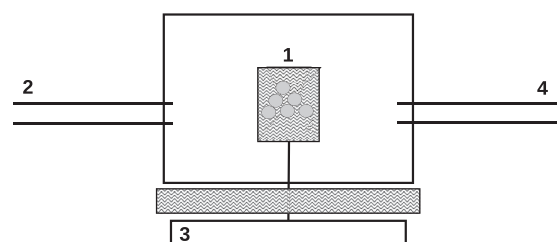


**Figure 10.** Schematic wire-mesh reactor (WR); 1, heated wire-mesh sample holder; 2, pre-defined reaction gas; 3, balance; 4, gas sampling.

**Table 5.** Properties of employed test reactor types in the pulverised coal characterisation under blast furnace conditions.

Method <sup>a</sup>	Blast temperature	Heating rate	Pressure	Residence time	Gas velocity	Particle velocity	Sample rates
	(°C)	(K/s)	(bar)	(ms)	(m/s)	(m/s)	(kg/h)
DTF	<1700	10 <sup>4</sup>	1–200	10–2000	< 10	< 1	5 × 10 <sup>-3</sup> –2
FR	<1800	10 <sup>4</sup> –> 10 <sup>5</sup>	1–20	20–3000	< 30	< 20	4 × 10 <sup>-4</sup> –0.06
IR	<1700	> 10 <sup>5</sup>	1	20–140	< 50	10–20	0.2–70
TGA	1000–2000 <sup>b</sup>	0.5	1	>100,000	< 1	c	≈ 1 × 10 <sup>-6</sup>
High pressure TGA	1000–2000 <sup>b</sup>	0.5	1–50	>100,000	< 1	c	≈ 1 × 10 <sup>-6</sup>
Inductive oven TGA	1000–2000 <sup>b</sup>	10 <sup>3b</sup>	1	>1000	< 1	c	≈ 1 × 10 <sup>-6</sup>
WR	<1500	10 <sup>4</sup>	1–70	2–>100,000	< 1	c	≈ 1 × 10 <sup>-6</sup>

<sup>a</sup>DTF, drop-tube furnace; FR, flow reactor; IR, injection rig; TGA, thermo-gravimetric analysis; WR, wire-mesh reactor.

<sup>b</sup>Estimate.

<sup>c</sup>Batch operation, sample size in kg/experiment.

depending on furnace size and purpose. Figure 6 shows a schematic DTF setup.

### Flow reactor

Flow reactors (FR) are either vertically or horizontally aligned and fuel particles are pneumatically shot through the reactor. Temperature, pressure, and residence time ranges are similar to those of DTFs [14, 39]. However, particle heating rates within FRs are higher than in DTFs and reach values between 10<sup>4</sup> and 10<sup>5</sup> K/s [48, 49, 53] due to an increased heat transfer attributed to the higher particle velocities. Sample mass flow rates are typically below 0.1 kg/h [14, 53]. Carrier gas flow rates can vary significantly, depending on reactor geometry and desired residence time. Figure 7 depicts a basic setup of FRs employed for the characterisation of coal.

**Table 6.** Advantages and disadvantages of the different characterisation methods for pulverised coal characterisation.

Method <sup>a</sup>	Advantages	Disadvantages
DTF	High temperatures High pressures Residence times	Heating rates Gas velocities Particle velocities
FR	High temperatures High heating rates High pressures Residence times	Particle velocities Gas velocities
IR	High temperatures High heating rates (high pressure) Residence times Sample size Gas velocities Particle velocities	Pressure (sample size)
TGA	Controlled environment	Low heating rates Low pressures Long residence times Gas velocities Stagnant particles Sample size
High pressure TGA	High pressures	Low heating rates Long residence times Gas velocities Stagnant particles Sample size
Inductive oven TGA	High heating rates	Low pressures Long residence times Gas velocities Stagnant particles Sample size
WR	High pressures	Gas velocities Stagnant particles Sample size Mesh effects

<sup>a</sup>DTF, drop-tube furnace; FR, flow reactor; IR, injection rig; TGA, thermo-gravimetric analysis; WR, wire-mesh reactor.

### Injection rig

Injection rigs (IR) are similar to FRs; however, they use coal mass flows orders of magnitude higher than FRs (0.2–150 kg/h) [18, 38, 43, 65]. Consequently, gas flow rates must also be significantly increased compared to FRs (up to several hundreds of N m<sup>3</sup>/h [34, 35]). The high velocities within IRs result in residence times between 20 and 140 ms [18, 36]. PC particles are continuously injected into a pre-heated combustion chamber surrounded by a pre-heated co-flow. The relative velocity at the injection point is at the same order of magnitude as in PC combustion. Therefore, heating rates within IRs are in the order of 10<sup>5</sup> K/s and above [36]. IRs used for PC characterisation are usually operated at ambient pressure due to the required gas flow rates. Particle sampling is done by sampling ports or at the end of the reactor. Figure 8 shows the basic IR components found in the literature.

Special IRs are operated in batch mode, performing single sample shots into a pre-heated chamber [18, 41–45]. These batch rigs often require sample masses in the range of several milligrams (10<sup>-6</sup> kg) [43].

### Thermo-gravimetric analysis

Thermo-gravimetric analysis (TGA) is a common, commercially available device, and is a default method for characterising gas–solid reaction kinetics or the characterisation of combustion and pyrolysis residues. Several specialised TGA appliances exist, including high-pressure TGAs or high-heating rate TGAs. Compared to the other employed reactor concepts, TGA heating rates are the lowest (ranging between 0.5 and 10<sup>3</sup> K/s [37, 46, 52]). Pressure and temperature ranges of up to 50 bars and 2000°C are possible for special TGA equipment. Residence times range from several seconds to minutes [44]. These long residence times are owed to the discontinuous batch-wise operation. Typical sample sizes are in the range of 10<sup>-6</sup> kg per experiment [37, 43, 46]. The gas–solid contact area is reduced, as samples are prepared in suitable crucibles. Some macro-TGAs are suitable for higher sample masses (≈ 10<sup>-3</sup> kg). Figure 9 illustrates a schematic setup of a typical TGA.

### Wire-mesh reactor

Sample holders in wire-mesh reactors (WR) are resistance-heated metal meshes. Therefore, the sample is fully perfused by the reaction gas. This configuration enables heating rates of around 10<sup>4</sup> K/s [59, 66], while temperatures are limited by oxygen partial pressures and the mesh material. Pressures of up to 70 bars and temperatures of up to 1600°C are reported in literature [60, 61, 66]. Residence times of 2 ms up to several seconds are possible [21, 66]. The main difference between FRs and WRs is that coal samples are fixed in

the wire mesh and, thus, solid residues stay there. Figure 10 depicts a generic WR setup.

### Comparison of characterisation methods

Table 5 summarises the collected operation parameters of the different reactor types. Only selected reactors are included, as this work focuses on metallurgical applications. Nevertheless, the obtained operating parameters enable evaluating the different reactor types in terms of their capabilities to reproduce blast furnace operating conditions. A thorough review of these reactor types showed that specially designed DTFs and FRs come close to the required conditions. Large IRs are typically operated at ambient pressure [18, 38, 43, 65], meaning pressure effects are neglected during IR tests. These IRs operate at solid fuel rates of several kg/h and gas flow rates in the range of  $10^2 \text{ Nm}^3/\text{h}$ . Therefore, operating an IR for screening tests of PC is assumed to be costly. Special small-scale IRs operate at higher pressures and smaller sample sizes [37, 43, 46]. Conversely, even high-heating-rate-inductive oven TGAs achieve low rates compared to blast furnace conditions. Residence times are several orders of magnitude higher in TGAs than in other reactor types and blast furnace raceway zones. WRs are limited to relatively low temperatures by the material of the heated sample holder. Moreover, WRs that are similar to TGAs operated in batch mode, thus, samples have long residence times in the hot oxidising atmosphere, which is contradictory to blast furnace conditions. In the blast furnace raceway zone, coal particles reach the reducing zone surrounding the tuyeres after approximately 20–30 ms [16–18].

Table 6 shows the advantages and disadvantages of the different characterisation methods with respect to the design criteria defined in Section 'Dependences of PC conversion'.

### Summary and conclusion

Diverse reactor types are currently employed for evaluating PCI across the world. Special drop-tube furnaces (DTF) and flow reactors (FR) are capable of reproducing similar conversion conditions as in the raceway zone, while others fail to provide reasonable results, e.g. thermo-gravimetric analysis (TGA) and wire-mesh reactors (WR). Larger injection rigs (IR) can simulate raceway zone conditions at ambient pressures, thus these IRs disregard the importance of the operating pressure on coal conversion [8]. The number of specialised DTFs/FRs is limited and testing capacity is low. Comparing results from different test rigs is not recommended, as there is no agreed-upon, standardised procedure for testing PC and, moreover, the different testing equipment characteristics differ (see Section 'Dependences of PC conversion').

The preceding discusses key parameters to provide similar conversion conditions in test equipment, as supported by a conceptual analysis of the coal conversion process. These parameters were defined as the conversion temperature, employed heating rates, and pressure, while the particle boundary layer or ambient gas phase is of lesser importance and can be calibrated. A suitable reactor concept for PC testing under blast furnace conditions and a testing protocol will be developed based on these findings. This could contribute to more efficient evaluation of PCI coals in terms of their conversion behaviour and energy release under blast furnace conditions with the final goal of finding PCI coals with optimal performance. An increased PCI injection level during the blast

furnace process would lead to decreased  $\text{CO}_2$  emissions of an integrated steel mill due to a reduced coke consumption and production. In addition, coking coals, which are essential to produce blast furnace coke for steel mills, represent a critical raw material with a limited global availability but a high economic importance [67, 68]. Increasing PCI injection rates would, therefore, decrease the dependence on the coking coal market.

The presented work partly contradicts the findings of Li et al. [6, 7], who postulated that DTFs can be used instead of IRs to characterise injection coals. Based on the thorough evaluation of the involved phenomena and additional literature, DTFs generally provide different results than IRs and, therefore, should not be employed for the evaluation of injection coals. The deviating operating conditions can significantly alter the evaluation results.

### Acknowledgements

The authors acknowledge the TU Wien University Library for financial support through its Open Access Funding Program.

### Disclosure statement

No potential conflict of interest was reported by the authors.

### Funding

This work is supported by the Österreichische Forschungsförderungsgesellschaft Grant Number 844607. The authors gratefully acknowledge the funding support of K1-MET GmbH, Metallurgical Competence Center. The research program of the competence center K1-MET is supported by COMET (Competence Center for Excellent Technologies), the Austrian program for competence centers. COMET is funded by the Federal Ministry for Transport, Innovation and Technology, the Federal Ministry for Science, Research and Economy, the province of Upper Austria, Tyrol, and Styria, the Styrian Business Promotion Agency.

### ORCID

Markus Bösenhofer  <http://orcid.org/0000-0003-3412-2113>  
Michael Harasek  <http://orcid.org/0000-0002-6490-5840>

### References

- [1] Remus R, Aguado-Monsonet MA, Roudier S, et al. Best available techniques (BAT) reference document for iron and steel production. European Commission Joint Research Centre Institute for Prospective Technological Studies (Report EUR 25521 EN) Luxembourg: Publications Office of the European Union. 2013; Industrial Emissions Directive 2010/75/EU:339–347.
- [2] Smoot LD, Smith PJ. Coal combustion and gasification. New York: Springer Science & Business Media; 1985.
- [3] Pratt DT, Smoot L, Pratt D. Pulverized coal combustion and gasification. New York: Springer Science & Business Media; 1979.
- [4] Szekeley J, Evans JW, Sohn HY. Gas–solid reactions. Cambridge (MA): Academic Press; 1976.
- [5] Steer JM, Marsh R, Morgan D, et al. The effects of particle grinding on the burnout and surface chemistry of coals in a drop tube furnace. *Fuel*. 2015;160:413–423.
- [6] Li H, Elliott L, Rogers H, et al. Reactivity study of two coal chars produced in a drop-tube furnace and a pulverized coal injection rig. *Energy Fuels*. 2012;26(8):4690–4695.
- [7] Li H, Elliott L, Rogers H, et al. Comparative study on the combustion performance of coals on a pilot-scale test rig simulating blast furnace pulverized coal injection and a lab-scale drop-tube furnace. *Energy Fuels*. 2014;28(1):363–368.

- [8] Wall TF, Liu G, Wu H, et al. The effects of pressure on coal reactions during pulverised coal combustion and gasification. *Prog Energy Combust Sci.* 2002;28(5):405–433.
- [9] Friedemann J, Baitalow F, Ceia T, et al. Experimentelle Untersuchungen zur Primärfragmentierung von Kohlepartikeln im Drop-Kalorimeter [Experimental investigation on primary fragmentation of coal particles in the drop-calorimeter]. *Chem Ing Techn.* 2014;86(10):1790–1796.
- [10] Friedemann J, Wagner A, Heinze A, et al. Direct optical observation of coal particle fragmentation behavior in a drop-tube reactor. *Fuel.* 2016;166:382–391.
- [11] Stanmore B, Brillard A, Gilot P, et al. Fragmentation of small coal particles under fluidized-bed combustor conditions. *Symp (Int) Combust.* 1996;26(2):3269–3275.
- [12] Fkyerat M, Hosseini E, Delfosse L, et al. Observed evolution of petrographic and textural features of coal particles, accompanying primary fragmentation during the earlier stages of combustion. *Symp (Int) Combust.* 1991;23(1):1223–1230. Twenty-Third Symposium (International) on Combustion.
- [13] Sasongko D, Stubington JF. Significant factors affecting devolatilization of fragmenting, non-swelling coals in fluidized bed combustion. *Chem Eng Sci.* 1996;51(16):3909–3918.
- [14] Kim JH, Kim RG, Kim GB, et al. Effect of coal fragmentation on PCI combustion zone in blast furnace. *Exp Therm Fluid Sci.* 2016;79:266–274.
- [15] Leonard JW, Humphreys KK. Coal preparation. American Institute of Mining, Metallurgical, and Petroleum Engineers, Wilkes-Barre, PA, USA; 1979.
- [16] Harasek M, Maier C, Jordan C, et al. Investigation of alternative reducing agent conversion in the raceway cavity of blast furnaces by numerical simulation. Proceedings AISTech 2016. Association Iron and Steel Technology; 2016. p. 14.
- [17] Maier C. Numerical modeling of the blast furnace process – injection of auxiliary reducing agents into the raceway [dissertation]. Institute of Chemical, Environmental, and Bioscience Engineering, Technische Universität Wien; 2015.
- [18] Babich A, Senk D, Born S. Interaction between co-injected substances with pulverized coal into the blast furnace. *ISIJ Int.* 2014;54(12):2704–2712.
- [19] Alonso M, Borrego A, Álvarez D, et al. A reactivity study of chars obtained at different temperatures in relation to their petrographic characteristics. *Fuel Process Technol.* 2001;69(3):257–272.
- [20] Thomas CG, Shibaoka M, Gawronski E, et al. Reactive (fusible) inertinite in pulverized fuel combustion: 2. Determination of reactive (fusible) inertinite. *Fuel.* 1993;72(7):913–919.
- [21] Cai HY, Kandyoti R. Effect of changing inertinite concentration on pyrolysis yields and char reactivities of two South African coals. *Energy Fuels.* 1995;9(6):956–961.
- [22] Côme GM. Gas-phase thermal reactions: chemical engineering kinetics. Boston: Springer Science & Business Media; 2013.
- [23] Rumpel S. Die autotherme Wirbelschichtpyrolyse zur Erzeugung heizwertreicher Stützbrennstoffe [Autothermal fluidized bed pyrolysis for the production of high heating value support fuels] [dissertation]. Faculty of Chemical and Process Engineering, Karlsruhe Institute of Technology; 2000.
- [24] Tepper H. Zur Vergasung von Rest- und Abfallholz in Wirbelschichtreaktoren für dezentrale Energieversorgungsanlagen [On the gasification of waste wood for the decentralised energy supply plants] [dissertation]. Faculty of Process and Systems Engineering, Otto-von-Guericke-Universität Magdeburg; 2005.
- [25] Froment GF, Bischoff KB, Wilde JD. Chemical reactor analysis and design. Hoboken (NJ): Wiley; 2010.
- [26] Mehrabian R, Zahirovic S, Scharler R, et al. A CFD model for thermal conversion of thermally thick biomass particles. *Fuel Process Technol.* 2012;95:96–108.
- [27] Thunman H, Leckner B, Niklasson F, et al. Combustion of wood particles – a particle model for Eulerian calculations. *Combust Flame.* 2002;129(1):30–46.
- [28] Baehr HD, Stephan K. Heat and mass transfer, Vol. 2. Berlin, Heidelberg: Springer-Verlag; 2006.
- [29] Fairbanks D, Wilke C. Diffusion coefficients in multicomponent gas mixtures. *Ind Eng Chem.* 1950;42(3):471–475.
- [30] Poling BE, Prausnitz JM, O'Connell JP, et al. The properties of gases and liquids, Vol. 5. New York: McGraw-Hill; 2001.
- [31] Di Blasi C. Kinetic and heat transfer control in the slow and flash pyrolysis of solids. *Ind Eng Chem Res.* 1996;35(1):37–46.
- [32] Bergman T, Lavine A, Incropera F, et al. Fundamentals of heat and mass. Hoboken (NJ): Wiley; 2011.
- [33] Goodwin DG, Moffat HK, Speth RL. Cantera: An object-oriented software toolkit for chemical kinetics, thermodynamics, and transport processes [<http://www.cantera.org>]; 2017. Version 2.3.0.
- [34] Mathieson JG, Truelove JS, Rogers H. Toward an understanding of coal combustion in blast furnace tuyere injection. *Fuel.* 2005;84(10):1229–1237.
- [35] Shen Y, Guo B, Yu A, et al. Three-dimensional modelling of coal combustion in blast furnace. *ISIJ Int.* 2008;48(6):777–786.
- [36] Mathieson JG, Rogers H, Somerville MA, et al. Reducing net CO<sub>2</sub> emissions using charcoal as a blast furnace tuyere injectant. *ISIJ Int.* 2012;52(8):1489–1496.
- [37] Machado JGMdS, Osório E, Vilela ACF. Reactivity of Brazilian coal, charcoal, imported coal and blends aiming to their injection into blast furnaces. *Mater Res.* 2010;13(3):287–292.
- [38] Ray S, Giroux L, MacPhee T, et al. Evaluation of PCI coals in new injection facility at CanmetENERGY-Ottawa. AISTech – Iron and Steel Technology Conference Proceedings; Vol. 1; 01; 2015. p. 926–937.
- [39] Vascellari M, Roberts DG, Hla SS, et al. From laboratory-scale experiments to industrial-scale CFD simulations of entrained flow coal gasification. *Fuel.* 2015;152:58–73.
- [40] Harris D, Roberts D, Henderson D. Gasification behaviour of Australian coals at high temperature and pressure. *Fuel.* 2006;85(2):134–142.
- [41] Babich A, Senk D, Fernandez M. Charcoal behaviour by its injection into the modern blast furnace. *ISIJ Int.* 2010;50(1):81–88.
- [42] Gudenau HW, Stoesser K, Denecke H, et al. Environmental aspects and recycling of filter dusts by direct injection or use of agglomerates in shaft furnaces. *ISIJ Int.* 2000;40(3):218–223.
- [43] Babich A, Gudenau HW, Senk D, et al. Experimental modelling and measurements in the raceway when injecting auxiliary substances. International BF Lower Zone Symposium; 2002. p. 25–27.
- [44] Babich A, Senk D, Gudenau HW. Effect of coke reactivity and nut coke on blast furnace operation. *Ironmak Steelmak.* 2009;36(3):222–229.
- [45] Babich A, Senk D, Born S. Conversion behavior by multiple injection into the blast furnace tuyere. Proceedings AISTech 2014; 2014. p. 795–804.
- [46] Sahu SG, Mukherjee A, Kumar M, et al. Evaluation of combustion behaviour of coal blends for use in pulverized coal injection (PCI). *Appl Therm Eng.* 2014;73(1):1014–1021.
- [47] Ariyama T. Combustion behavior of pulverized coal in tuyere zone blast furnace and influence of injection lance arrangement on combustibility. *ISIJ Int.* 1994;34(6):476–483.
- [48] ECN. Lab-scale combustion/gasification simulator (LSC) – application and features 2009/2010 [Brochure]; 2010.
- [49] ECN. Lab scale combustion simulator (LSC) [Brochure]; 2017.
- [50] Adamczyk WP, Szlęk A, Klimanek A, et al. Design of the experimental rig for retrieving kinetic data of char particles. *Fuel Process Technol.* 2017;156:178–184.
- [51] Adamczyk WP, Bialecki R, Katelbach-Wozniak A, et al. A method for retrieving char oxidation kinetic data from reacting particle trajectories. Proceedings of the 8th European Combustion Meeting; 2017. p. 2621–2624.
- [52] Cores A, Babich A, Muñoz M, et al. Iron ores, fluxes and tuyere injected coals used in the blast furnace. *Ironmak Steelmak.* 2007;34(3):231–240.
- [53] Rubiera F, Arenillas A, Arias B, et al. Modification of combustion behaviour and NO emissions by coal blending. *Fuel Process Technol.* 2002;77–78:111–117.
- [54] Rubiera F, Arenillas A, Arias B, et al. Combustion behaviour of ultra clean coal obtained by chemical demineralisation. *Fuel.* 2003;82(15–17):2145–2151.
- [55] Faúndez J, Arenillas A, Rubiera F, et al. Ignition behaviour of different rank coals in an entrained flow reactor. *Fuel.* 2005;84(17):2172–2177.
- [56] Ökvist LS, Hyllander G, Olsson ET, et al. Injection of pulverized materials into the blast furnace raceway. 6th International Congress on the Science and Technology of Ironmaking 2012, ICSTI 2012; Vol. 3; 2012. p. 1721–1731.
- [57] Du SW, Chen WH, Lucas JA. Pulverized coal burnout in blast furnace simulated by a drop tube furnace. *Energy.* 2010;35(2):576–581.



- [58] Cloke M, Lester E, Thompson AW. Combustion characteristics of coals using a drop-tube furnace. *Fuel*. 2002;81(6):727–735.
- [59] Gibbins-Matham J, Kandiyoti R. Coal pyrolysis yields from fast and slow heating in a wire-mesh apparatus with a gas sweep. *Energy Fuels*. 1988;2(4):505–511.
- [60] Guell AJ, Kandiyoti R. Development of a gas-sweep facility for the direct capture of pyrolysis tars in a variable heating rate high-pressure wire-mesh reactor. *Energy Fuels*. 1993;7(6):943–952.
- [61] Wu L, Paterson N, Dugwell D, et al. Simulation of blast-furnace tuyere and raceway conditions in a wire mesh reactor: extents of combustion and gasification. *Energy Fuels*. 2007;21(4):2325–2334.
- [62] Murphy JJ, Shaddix CR. Combustion kinetics of coal chars in oxygen-enriched environments. *Combust Flame*. 2006;144(4):710–729.
- [63] Mitchell RE. Experimentally determined overall burning rates of coal chars. *Combust Sci Technol*. 1987;53(2–3):165–186.
- [64] Fletcher TH, Hardesty DR. Compilation of Sandia coal devolatilization data: milestone report. Livermore, CA, USA: Combustion Research Facility, Sandia National Laboratories, Livermore, CA, USA; 1992.
- [65] Tamura M, Watanabe S, Komaba K, et al. Combustion behaviour of pulverised coal in high temperature air condition for utility boilers. *Appl Therm Eng*. 2015;75:445–450.
- [66] Roberts DG, Ilyushechkin AY, Harris DJ. Linking laboratory data with pilot scale entrained flow coal gasification performance. Part 1: laboratory characterisation. *Fuel Process Technol*. 2012;94(1):86–93.
- [67] European Commission. Report on critical raw materials for the EU – Report of the ad hoc working group on defining critical raw materials. European Commission; May 2014.
- [68] European Commission. On the 2017 list of Critical Raw Materials for the EU. European Commission; September 2017.